Design of Cooling System for Electronic Devices Using Impinging Jets

Po Ting Lin[1*], Ching-Jui Chang[2], Huan Huang[3], and Bin Zheng[4]
[1]Rutgers, The State University of New Jersey, Mechanical and Aerospace Engineering, [2]FTR Systems (Shanghai) Inc., [3]PolarOnyx, Inc., [4]University of Electronic Science and Technology of China, School of Mechatronics Engineering.
*Corresponding author: 98 Brett Road, Piscataway, New Jersey 08854, USA, potinglin223@gmail.com

Abstract: The heat sink designs using impinging liquid jets, which form stagnation flows, feature uniform heat transfer coefficients, and provide thin thermal boundary layers, are studied to reduce the heat from GPUs. Three different designs using central, micro, and uniform-cross-section (UCS) central jets are studied and simulated in COMSOL. The efficiency factors, defined as the ratio of total removed energy over inlet pumping energy, are measured to quantitatively represent the heat transfer performances. The central and micro jet designs consume smaller amounts of pumping powers but form vortexes and thicker thermal boundary layers near the outlets. The UCS central jet design not only avoids the vortex formations but also maintains the thermal boundary layer thickness; therefore, higher efficiency has been achieved.

Keywords: impinging jet, CPU/GPU cooling, stagnation flow, computational fluid dynamics, thin thermal boundary layer.

1. Introduction

System cooling has become a major problem in designing and operating equipment used in a variety of industries, such as aerospace, nuclear, and electronics. Recently, in the electronic industry, the need for rapid cooling on the integrated circuits (ICs) keeps increasing due to the increasing number of transistors in the ICs which generate considerable amount of heat. Furthermore, while the refinement of manufacturing techniques, the sizes of the computer ICs are dramatically reduced. Thus, the heat flux on the chips is keeping climbing in a startling rate. Moreover, the sizes of the electronic devices are reduced to meet the market's needs. As a result, the available space for cooling system is very limited and the convectional cooling techniques cannot satisfy the increasing needs.

Earlier in the end of last century, forced convection cooling systems replaced natural convection systems on computer chips to improve the low efficiency in the latter one. Furthermore, the literature review [1] and experiments [2-3] showed the forced convection cooling systems, including air and liquid cooling technologies, provide higher power dissipation capabilities. There are three major techniques to improve the efficiency of dissipating the heat from the computer components utilizing the air cooling systems: changing the geometry of the conducting material to increase convection surface area, changing the conducting material to increase the surface temperature and achieve higher convection coefficient, and, lastly, increasing the flow rate of the external fluid to reduce the thermal and hydraulic boundary layers.

However, increasing the surface area increases the cost in terms of using more materials for more complicated manufacturing processes for the conductive fins. Changing the more conductive material such as copper often increases the costs and the difficulties of fabrication processes. Increasing the flow rate usually requires larger fans which occupy valuable spaces and generate annoying noises. Furthermore, frequent maintenance was usually required for air cooling systems, such as lubricating the bearing of the fans and cleaning the dust accumulated over time. Therefore, we mainly focus on the development of the liquid cooling systems in this paper and intend to design the next-generation cooling system for electronic devices.

Facing the increasing need for faster and larger computations in the recent engineering technologies, the frequency of the processing unit has become higher but its size has become smaller, that is, extensively increasing heat per area. Furthermore, the latest designs of the personal computers (PCs) or the servers tend to decrease their sizes resulting in limited working

spaces for the computer components, such as central and graphics processing units (CPUs and GPUs), and the cooling apparatuses for them. The conventional cooling systems such as heat sink and fans cannot satisfy the needs for high performances and efficiency, especially for the GPU in PC which only has very restricted area for cooling devices. To this end, the liquid cooling system provides an efficient and compact solution in terms of higher conductivity, lower requirement of flow rate, and less noise.

In the liquid cooling, the stagnation flows provide higher heat efficiency [4-5] due to the characteristics of thin thermal and hydraulic boundary layers. Therefore, three different cooling systems using liquid impinging jets are designed and studied in this paper. The first kind utilizes single impinging jet at the center of the heat sink while the second one uses multiple jets. In the first two designs, the vortexes are formed decreasing the thermal efficiency of cooling. The last design considers a uniform cross-section channel for the single impinging flow in order to avoid the vortex formations and improve the thermal efficiency. The COMSOL multiphysics software is utilized to numerically analyze and simulate the three liquid cooling systems while multiple physics domains including conduction heat transfer, convection heat transfer, and fluid dynamics are involved.

2. Design of Liquid Cooling Systems

In this section, the design considerations of the liquid cooling systems are presented. The first subsection defines the cooling problems of CPU or GPU using the designs of liquid cooling systems. Furthermore, the numerical methods as well as the boundary conditions for the cooling systems are defined. To simplify the problem, the conduction is decoupled from the multiple physics domains and the detailed information is further discussed.

2.1 Cooling Problems of Electronic Devices

In this paper, the liquid heat sinks are designed for the cooling of GPUs and they are also applicable for other heat-generating electronic devices such as CPUs. The cooling apparatus is directly attached on top of the GPUs which is the main source of the heat generation while the bottom of the heat sink spreads the heat via conduction heat transfer. The material property of the heat sink is greatly related to the performance of the conduction. The liquid coolant flows through the top surface of the heat sink and carries the heat away via convection heat transfer. The geometry of the heat sink, which not only varies the flow behavior but also affects the thermal efficiency of cooling, is another significant factor in the design of liquid cooling systems.

The chip size of the GPU is considered as $14 \times 14\ \mathrm{mm}^2$ while the working area for the heat spreader is considered as $39 \times 39 \times 18\ \mathrm{mm}^3$ due to the common limited spaces in computers. Figure 1 illustrates the model of the liquid cooling system for a GPU chip. In the figure, the black rectangular plate represents the GPU chip and the brown case is the design of the heat spreader, which has the inner dimension of $35 \times 35 \times 13\ \mathrm{mm}^3$. Some circular holes are drilled on the top of the heat spreader as the inlets and outlets of liquid coolant as the flow directions are illustrated by the blue arrows. Due to the geometrical symmetry of the design, only a part of the design space, illustrated by the dashed pentahedron, is modeled and studied in COMSOL with appropriate boundary conditions.

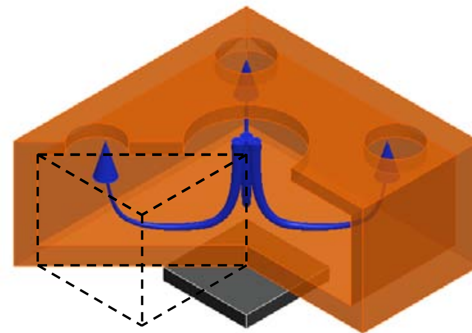

Figure 1. A drawing of the liquid cooling system.

2.2 Numerical Methods

Multiple physics phases are considered in the pentahedral design domain, including the solid conductive area at the bottom and the liquid convective region for the rest. There are 11 different surface regions in the model of the cooling system, illustrated in Figure 2. The surface regions *A* and *D* represent the interfaces between the coolant and the cold wall; the

surfaces E and K are the boundaries between symmetric fluid domains; the circular regions C and G respectively indicates the outlet and inlet of coolant; lastly, the rest of the surfaces are the conductive boundaries in the heat spreader while the surface I is constantly heated by the GPU chip.

Furthermore, the boundary conditions are reconstructed and listed in Table 1. Note that the boundary A is considered as insulation to neglect the end effect. The actual temperature of the fluid out of the model should be expected to be slightly higher. In CPU or GPU, the power consumption is usually a constant value so that a steady working state of the heat generated by the chips is assumed to be a constant. The heat flux q_0 of GPU is defined as a constant value of 25 W/cm^2 to simplify the problem. The flow is driven by the pressure difference between the inlet and the outlet and the pressure drop is defined as 20 Pa. Copper is used as the spreader material because of the characteristic of high conductivity.

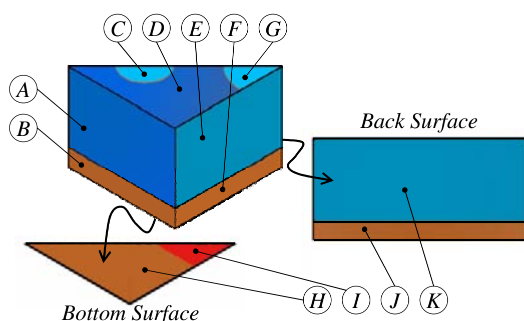

Figure 2. Illustrations and IDs of the surface regions in the pentahedral design domain.

Table 1. Boundary conditions in Figure 2.

ID	Fluidic	Convection	Conduction
A	No slip	Insulation	–
B	–	–	Insulation
C	Outflow	Convective flux	–
D	No slip	Insulation	–
E	Slip	Insulation	–
F	–	–	Insulation
G	Inflow	T_0 = 300 K	–
H	–	–	Insulation
I	–	–	Constant heat flux
J	–	–	Insulation
K	Slip	Insulation	–

2.3 Further Simplifications

Three physics domains are coupled in the pentahedral design model. Although only a part of the whole model is selected for analysis, it is still costly to calculate the numerical results. Further simplifications on the boundary conditions need to be made to reasonably decouple the problem. The first attempt is to decouple the heat conduction in the solid part from the physics acting in the fluid if some evidences can be found to justify this idea. That is, if constant temperature on the fluid-heat spreader interface can be assumed, the conduction domain can be decoupled form the problem.

The numerical result in Figure 3 shows that the conductivity of copper is sufficiently high such that only slight temperature difference (around 1.5 K) can be found at the interface between the water and the copper heat spreader. Furthermore, the finite element analysis tends to over-estimate the temperature at the sharp corners with higher temperature gradients due to the computational singularities of interpolations from near points. Therefore, the temperature difference can be considered as less than 1.5 K, which supports the idea of treating the bottom copper heat spreader as constant temperature. It saves a lot more computational powers by reducing the three-physics domain into a two-physics design problem and considering constantly heated wall at the bottom surface of the heat sink. In the further simulation, the heat spreader temperature is fixed at 350 K.

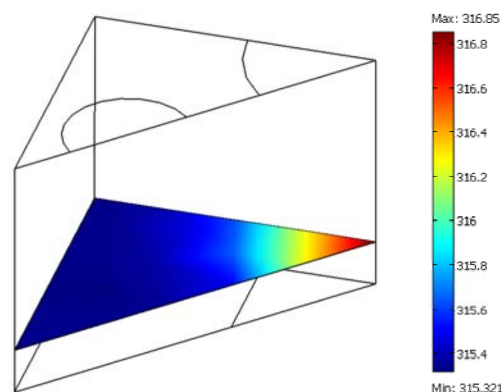

Figure 3. Nearly constant temperature is found at the water-copper interface as P_0 = 0 Pa, P_{in} = 20 Pa, T_0 = 300 K, and q_0 = 25 W/cm^2.

3. Detailed Information and Numerical Results

In the paper, three different geometries are studied. They are the central impinging jet, the micro impinging jet and the alternative central jet designs. The design variables and results are presented and discussed in this section. An efficiency factor is defined to quantitatively represent the heat transfer performances.

3.1 Design I: Central Impinging Jet

In the central impinging jet design shown in Figure 1, different dimensions of inlets and outlets have been examined. In order to maintain constant pressure drop from inlet to outlet, the dimensions are subjected to the constant total volume flow rate, 10 liter per hour. The inlet radius r_{in} is chosen as the design variable and the outlet dimension is calculated accordingly. A typical numerical result is shown in Figure 4. The top subfigure shows the streamline and the formation of vortex inside the while the bottom subfigure shows the temperature distribution. The thermal boundary layer at the bottom is fairly thin at the beginning when the flow comes in and grows thicker as the liquid flows out.

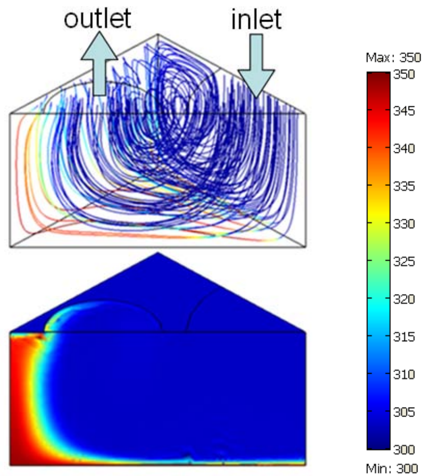

Figure 4. Streamline and temperature distribution in the central jet design.

To investigate the performances of heat sink designs with different inlet dimensions, a heat transfer efficiency factor is defined as the ratio of the total heat flux at the fluid-solid interface and the total exhausted power of the pump. The utilized power of pump to maintain the constant volume flow rate in the control volume is calculated by the product of the total pressure difference between inflow and outflow. Therefore, the heat transfer efficiency E is given by:

$$e = \frac{\int q'' dA_{base}}{\Delta p \cdot A_{in} \cdot V_{in}} \quad (1)$$

The results of different designs are listed in Table 2. When the inlet radius decreases, stronger vortexes are formed to help the heat transfer from the spreader to the fluid; however, larger pumping power is required to maintain the total volume flow rate. As a result, central jet design with smaller inlet radius is capable of releasing more energy from the heat spreader but less efficient than the design with larger radius.

Table 2. The design parameters and results for central jet design.

r_{in} (mm)	V_{in} (mm/s)	$\int q'' dA_b$ (w)	$\Delta p \cdot A_{in}$ (N)	e
6	24.56	10.746	3.291e-6	1.329e5
8	13.82	9.473	1.740e-6	3.941e5
10	8.84	7.848	1.582e-6	5.613e5

3.2 Design II: Micro Impinging Jets

Another geometry design of the conducting media is an array of micro-jets, vertically flushing the bottom copper heat spreader and acting as stagnation flows. The objective of the micro-jet design is to take advantage of the specific characteristic of constant heat transfer rate at the stagnation point and expect to find optimal heat transfer efficiency. Similarly, the design variable is the inlet radius. Since the numbers of inlets and outlets remain the same, the inlet radius equals the outlet radius in order to maintain the constant volume flow rate, 10 liter per hour.

On the top of the fluid domain, a number of micro jets are designed as shown in Figure 5 with a pitch of 5 mm. Eighteen inlets and eighteen outlets are arranged in an interlaced arrangement. Therefore, the inflows act consistently with each other, as well as the outflows. The flow motions are found symmetric so that only a pentahedron shown in Figure 5 is needed to analyze the fluid dynamics

and thermal behavior for the entire fluid domain. Due to the symmetry, the boundary conditions of the side walls are slipping / symmetric. The top and bottom surfaces are no-slipping. The boundary condition at the inlet is considered as zero-normal-pressure. The copper heat spreader is considered as a constant temperature wall of 350 K as described previously. The variations at the sides of the fluid domain are neglected. Due to the symmetry, the side walls of the pentahedron are considered as heat insulated (i.e. no heat exchange between two pentahedron of fluid). The top surface is set as constant temperature of 300 K, as well as the thermal boundary condition at the inlet. The outlet is set as convective flux.

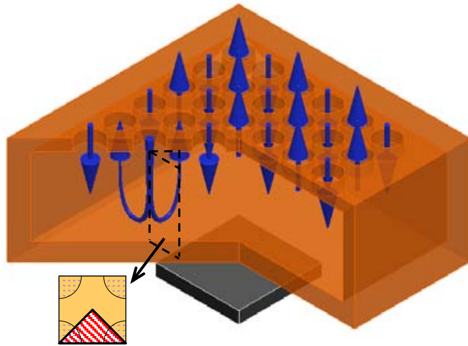

Figure 5. A drawing of the micro-jet design. (The pentahedron, the red-hatched region, is chosen to be the design domain.

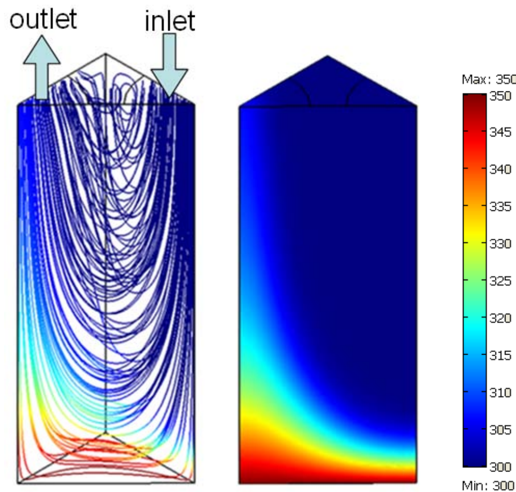

Figure 6. A typical result of streamlines and boundary temperature profiles in the micro jet design.

Several different radiuses of inlets and outlets are designed and modeled. A typical result of this design is shown in Figure 6. The left subfigure shows the vortex in the design domain while the right subfigure shows the boundary temperature profile. The thermal boundary layer is fairly thin throughout the cooling device. Due to the manufacturing limitation, the radius is limited in a bound between 0.2 and 2.3 mm (i.e. the holes of inlets and outlets cannot be less than 0.2 mm; the gaps between the holes cannot be less that 0.2 mm).

In Table 3, the resultant total heat fluxes at the fluid-solid interface are found in different radiuses. As the size of the inlet increases, the relative inlet velocity increases, as well as the pressure difference. As a result, the exhausted power of the pump increases gradually. Although the total heat flux increases due to the higher stream velocity, a huge amount of the energy is exhausted by the shear forces from the vortexes. In general, the increment of the inlet size will enhance the heat transfer efficiency. However, too large inlet size slows down the stream velocity resulting in a great drop of the total heat flux. The radius of 2 mm is found to be the most efficient design for the micro-jet cooling system.

Table 3. The results of micro-jet designs with different radius.

r_{in} (mm)	V_{in} (mm/s)	$\int q^{''} dA_b$ (w)	$\Delta p \cdot A_{in}$ (N)	e
0.2	1.228	1.165	1.397e-5	6.791e4
1	4.912e-2	2.759e-1	6.167e-7	9.108e6
1.5	2.183e-2	1.550e-1	2.789e-7	2.546e7
2	1.228e-2	7.865e-2	1.300e-7	4.928e7
2.3	9.286e-3	4.160e-2	1.530e-7	2.929e7

3.3 Uniform-Cross-Section (UCS) Central Jet

From the previous two designs, the fluid forms vortexes in the control volume which dissipate unnecessary lost of energy on shear stresses and decrease the efficiency of heat transfer. Furthermore, the thickness of the thermal boundary layers is not uniform especially at the outlet positions where the heat transfer rates are low.

The third design is to use an uniform cross section of the flow channel to decrease and maintain the thickness of the thermal boundary

layer throughout the bottom surface such that the temperature gradient is increased near the boundary. With increased temperature gradient, the heat flux is therefore increased. Furthermore, by the design of the geometry, the vortex is reduced so that all the pump work is mainly used to propel the fluid against the wall shear only. In order to minimize the frustrations of the fluid generated by the geometry, the device is designed to have uniform cross section area along the fluid flowing path. The thickness of the opening on the control volume is indicated in Figure 7. The height on the curve is governed by the flowing equation:

$$h = \frac{A_{inlet}}{A_{flow_band}} = \frac{\pi r_{inlet}^2}{2\pi r_x} \qquad (2)$$

where r_x is the distance of the position away from center.

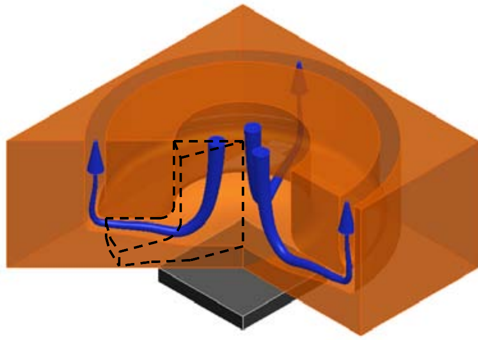

Figure 7. A drawing of the uniform-cross-section central jet design that has fluid coming in the central opening and flow out toward the side with uniform flow intersection.

A control volume base on a slice of the fluid domain of 10 degree out of a full revolution is selected since this design is axisymmetric. For thermal analysis, the upper surfaces are considered to be the same temperature as the inflow stream (300K), the bottom surface is set to be a constant temperature (350K), the outlet is set to be convective flux, and both sides are configure d to be insulated. For hydrodynamic analysis, the inlet pressure is set to be a constant, the outlet is configure d to have a constant flow velocity calculated base on the given system flow rate and the inlet radius, the both sides adjoint to fluid are set to slip/symmetric and the surfaces adjoint to solid parts are specified to be the wall against the fluid. A typical result of this design is shown in Figure 8. The thermal boundary layer is uniformly thin throughout the entire heat exchange surface. The total heat transferred by this design is extremely high because the thermal boundary is extremely thin and the temperature gradient is considerable high.

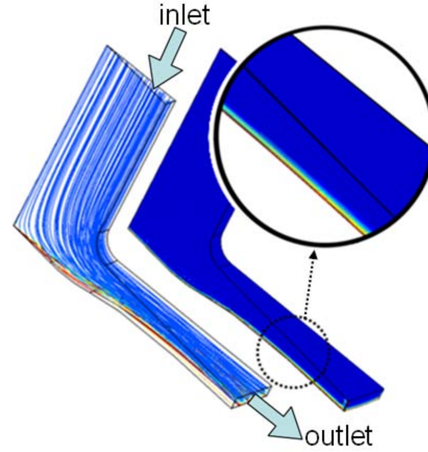

Figure 8. A typical result of streamlines and temperature profiles in the UCS central jet design.

Five different designs of varying the radius of the inlet from 3mm to 7mm are carried out and the results are shown in Table 4. The pump efficiency is calculated using the equation aforementioned. It is worth notice that this design has the fluid in it behavior as laminar while the other two designs have turbulent. From the results shown above, it can be noticed that the efficiency varies with the inlet radii. Under the same amount of flow rate, the optimal efficiency is expected larger than 7mm of the inlet radius. However, the heat transfer rate is dropping to a level that can not be well utilized. Although it requires more pressure difference to drive the fluid because of the extra contacting

Table 4. The results of UCS central jet design with different radius.

r_{in} (mm)	V_{in} (mm/s)	$\int q'' dA_b$ (w)	$\Delta p \cdot A_{in}$ (N)	e
3	9.229e-2	7.215	3.569e-5	2.191e6
4	5.529e-2	5.186	1.094e-5	8.570e6
5	3.539e-2	3.368	4.519e-6	2.106e7
6	2.457e-2	2.491	2.571e-6	3.943e7
7	1.805e-2	1.887	1.810e-6	5.774e7

surface area comparing to the first two designs in this paper, this design is very thermally efficient considering the total releasing heat. Better results can be expected with higher flow rate.

4. Conclusion

Liquid based cooling devices using impinging jets are designed and studied in this paper because a jet against a wall forms a thin hydrodynamic boundary layer as well as a thin thermal boundary layer which improves heat dissipation tremendously. Three different designs of geometries are carried out in this paper and their cooling efficiency against pump power consumption is studied. The first two designs consumes smaller amount of pump power because they have fewer liquid/solid interface area. Vortexes are found in these two designs due to the geometry and the turbulent models are used to obtain the result. The thermal and hydrodynamic boundary layers distort much in the design control volume. The third design tries to confine the fluid in a uniform-cross-section channel to minimize the boundary layers and avoid the appearance of the vortexes. This design can use fewer amount of flow rate to achieve high thermal efficiency. Lastly, the detailed comparisons of the numerical results of three different heat sink designs are given in the Figure 9. In general, smaller inlet dimensions provide higher total removed energy but require larger pumping energy at the inlet. In the subfigure (c), the UCS central jet design has higher thermal efficiency while the central jet design has the lowest.

5. References

1. Incropera, F.P., Convection Heat-Transfer in Electronic Equipment Cooling, *Journal of Heat Transfer-Transactions of the Asme*, **110**, page 1097-1111 (1988)
2. Sparrow, E.M., J.E. Niethammer, and A. Chaboki, Heat transfer and pressure drop characteristics of arrays of rectangular modules encountered in electronic equipment, *International Journal of Heat and Mass Transfer*, **25**, page 961-973 (1982)
3. Sparrow, E.M., S.B. Vemuri, and D.S. Kadle, Enhanced and local heat transfer, pressure drop, and flow visualization for arrays of block-like electronic components, *International Journal of Heat and Mass Transfer*, **26**, page 689-699 (1983)
4. Cengel, Y.A., *Heat Transfer: A Practical Approach*. McGraw Hill, New York, NY, USA (1998)
5. Incropera, F.P., *Liquid Cooling of Electronic Devices by Single-Phase Convection*. John Wiley & Son, Danvers, MA, USA (1999)

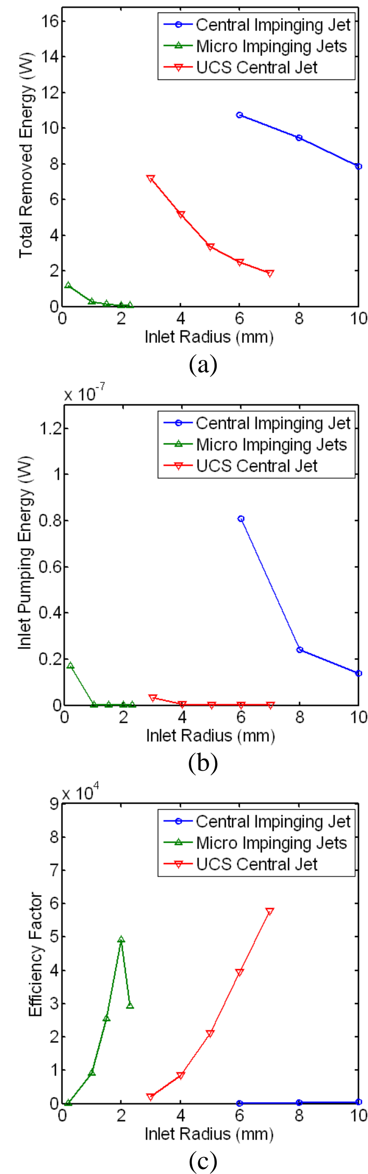

Figure 9. Comparisons of three different heat sink designs: (a) total removed energy; (b) inlet pumping energy; (c) efficiency factor.